Applications of Physiologic Pharmacokinetic Modeling in Carcinogenic Risk Assessment

Daniel Krewski,[1,2] James R. Withey,[1] Lung-fa Ku,[1] and Melvin E. Andersen[3]

[1]Health Protection Branch, Health and Welfare Canada, Ottawa, Ontario, Canada; [2]Department of Mathemetics and Statistics, Carleton University, Ottawa, Ontario, Canada; [3]Chemical Industry Institute of Toxicology, Research Triangle Park, North Carolina

The use of physiologically based pharmacokinetic (PBPK) models has been proposed as a means of estimating the dose of the reactive metabolites of carcinogenic xenobiotics reaching target tissues, thereby affording an opportunity to base estimates of potential cancer risk on tissue dose rather than external levels of exposure. In this article, we demonstrate how a PBPK model can be constructed by specifying mass-balance equations for each physiological compartment included in the model. In general, this leads to a system of nonlinear partial differential equations with which to characterize the compartmental system. These equations then can be solved numerically to determine the concentration of metabolites in each compartment as functions of time. In the special case of a linear pharmacokinetic system, we present simple closed-form expressions for the area under the concentration–time curves (AUC) in individual tissue compartments. A general relationship between the AUC in blood and other tissue compartments is also established. These results are of use in identifying those parameters in the models that characterize the integrated tissue dose, and which should therefore be the primary focus of sensitivity analyses. Applications of PBPK modeling for purposes of tissue dosimetry are reviewed, including models developed for methylene chloride, ethylene oxide, 1,4-dioxane, 1-nitropyrene, as well as polychlorinated biphenyls, dioxins, and furans. Special considerations in PBPK modeling related to aging, topical absorption, pregnancy, and mixed exposures are discussed. The linkage between pharmacokinetic models used for tissue dosimetry and pharmacodynamic models for neoplastic transformation of stem cells in the target tissue is explored. — Environ Health Perspect 102(Suppl 11):37–50 (1994)

Key words: pharmacokinetic model, pharmacodynamic model, tissue dosimetry, carcinogenic risk assessment

Introduction

Pharmacokinetics is the study of the absorption, distribution, metabolism, and elimination of xenobiotic agents in biologic systems. By studying the fate of xenobiotics upon entering the body, it is possible to obtain information on the amount of both the parent compound and reactive metabolites reaching tissues that may be targets for the induction of cancerous lesions. This affords an opportunity to incorporate data on tissue dose into pharmacodynamic models of carcinogenesis.

Considerable experience has now accumulated with the development of physiologically based pharmacokinetic (PBPK) models to describe the disposition of carcinogenic xenobiotics. Each compartment in a PBPK model represents a physiologically defined component of the body, such as blood or specific organs and tissues. Physiologic parameters such as body weight, blood flow rates, and tissue volumes are used to characterize the distribution of xenobiotics within the structure provided by the PBPK model; biochemical parameters such as partition coefficients govern uptake within target tissues. Metabolism in the liver or other tissues is generally described by first-order or Michaelis–Menten kinetics. PBPK models capable of accurately describing chemical disposition within mammalian systems have been developed for at least 15 chemical substances (*1*).

Traditional methods for predicting potential carcinogenic risk in humans from animal data involve a number of empirical assumptions (*2*). First, for low levels of exposure, it is generally assumed that carcinogenic risk is directly proportional to the level of exposure. Second, it is assumed that humans are at least as sensitive as the most sensitive animal species. In addition, interspecies scaling of carcinogenic potency is done in relation to body surface area or body weight, or an intermediate scaling factor (*3,4*). And third, it is tacitly assumed that the dose of the proximate carcinogen reaching the target tissue is proportional to the level of exposure to the parent compound. It should be noted, however, that classic pharmacokinetic and biochemical studies have indicated that some metabolic pathways are saturable, even at low levels of exposure. This phenomenon could give rise to a nonlinear dose–response relationship with a biochemical threshold.

The comparatively recent application of PBPK modeling to predict the dose of the proximate carcinogen delivered to the target tissue obviates the need to rely on empirical assumptions in carcinogenic risk assessment. In particular, PBPK models provide a basis for a more biologically based approach to dose, route, and species extrapolation. While physiologic modeling thus provides a more rational approach to risk assessment, there may be a number of uncertainties associated with its use since a moderately large number of parameters, each subject to some degree of error, are required for risk assessment applications.

The purpose of this article is to review the collective experience to date in developing PBPK models for carcinogenic chemicals, with a view to evaluating their role as a tool for obtaining more accurate predictions of carcinogenic risk through improved tissue dosimetry. We begin with a step-by-step overview of the process of building a PBPK model, defined in terms of mass–balance equations for individual compartments included in the model ("Development of a PBPK Model"). Appropriate measures of tissue dose are dis-

This article was presented at the Workshop on Pharmacokinetics: Defining the Dose for Risk Assessment held 4–5 March 1992 at the National Academy of Sciences in Washington, DC.

Address correspondence to Dr. Daniel Krewski, Health Protection Branch, Health and Welfare Canada, Ottawa, Ontario, Canada K1A OL2. Telephone (613) 954-0164. Fax (613) 952-9798.

cussed in "Tissue Dosimetry." Because PBPK models may involve in excess of 20 or more parameters, we review recent investigations designed to identify those parameters to which predictions of tissue dose are most sensitive ("Sensitivity Analysis"). The use of PBPK models developed to describe the fate of methylene chloride, styrene, ethylene oxide, 1,4-dioxane, 1-nitropyrene, as well as polychlorinated biphenyls, dioxins, and furans is reviewed in "Applications of PBPK Modeling." Special considerations in the application of PBPK models are discussed in "Other Considerations in Applications of PBPK Models," including the effects of aging, topical adsorption in inhalation studies, pregnancy, and exposure to complex mixtures. The linkage between pharmacokinetic models used for tissue dosimetry and pharmacodynamic models of carcinogenesis is explored in "Pharmacodynamics."

Development of a PBPK Model

A PBPK model envisages the body as being comprised of physiologically similar compartments. Each compartment represents an organ or tissue group, and linked to the central blood compartment by arterial and venous blood flow. The model is characterized by physiologic parameters such as tissue volumes and blood flow rates, biochemical parameters such as the partition coefficients, and kinetic parameters for metabolism and removal. These parameters are used to provide a mathematical description of the model using mass–balance equations for individual compartments.

General Organ Compartment

Consider first the general organ shown in Figure 1. A xenobiotic that has been taken up by the body and entered the bloodstream may enter the compartment through the arterial blood and leave through the venous blood. In certain compartments, the compound may enter or leave the compartment directly by nonarterial routes. For example, a compound could be removed from the liver by metabolism or from the kidneys by excretion. Compartment kinetics can be represented by the mass–balance equation:

$$\frac{\partial}{\partial t}C_I(t) = (Q_i/U_i)(C_b(t) - V_i(t)) + (1/U_i)\frac{\partial}{\partial t}Y_i(t) - (1/U_i)\frac{\partial}{\partial t}Z_i(t). \quad [1]$$

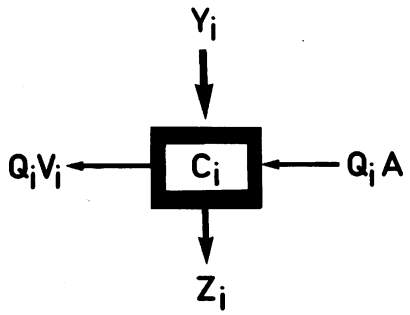

Figure 1. Schematic diagram of a general organ compartment: $C_i(t)$ = concentration of xenobiotic in tissue i at time t; Q_i = blood flow rate; U_i = tissue volume; A(t) = concentration of xenobiotic in arterial blood; $V_i(t)$ = concentration of xenobiotic in venous blood; $Y_i(t)$ = amount of xenobiotic directly entering compartment; $Z_i(t)$ = amount of xenobiotic directly removed from compartment.

Note that the concentration in the arterial blood is the same in all compartments. The allometric parameters such as tissue volume and blood flow rate involved in this equation are generally obtained by referring to published reference values (*5*).

Many PBPK models regard tissue uptake of chemical to be flow limited (*6*). It assumes that the venous blood from the tissue is in equilibrium with chemical in the tissue. This condition is related to the partition coefficient between tissue and blood. So

$$V_i(t) = C_i(t)/P_i, \quad [2]$$

where P_i denotes the partition coefficient between tissue and blood. The partition coefficient represents the ratio of the concentration of the compound in the tissue relative to that in blood under steady-state conditions.

For some compounds like 2,3,7,8-tetrachlorodibenzo-*p*-dioxin (TCDD), the ability of the tissue to retain the compound is limited by the availability of specific binding media such as protein. In this event, the linear relationship in Equation 2 must be replaced by a more complicated one allowing for saturation of protein binding (*7*).

The term $\partial Y_i(t)/\partial t$ represents the rate at which the compound enters the compartment directly. This can occur in blood or skin at time t_0 with intravenous or dermal exposure. Direct entry with a single exposure can be represented by the Dirac delta function:

$$\frac{\partial}{\partial t}Y_i(t) = \delta(t), \quad [3]$$

where $\partial(t) = 1$ for $t = t_0$ and is 0 otherwise. Continuous infusion from time t_1 to t_2 is represented by a step function with

$$\frac{\partial}{\partial t}Y_i(t) = \begin{cases} 1 & t1 \le t \le t2 \\ 0 & \text{otherwise.} \end{cases} \quad [4]$$

First-order absorption following a single exposure at time $t = 0$ is represented by: where $k_a > 0$ represents the kinetic rate coefficient for absorption.

$$\frac{\partial}{\partial t}Y_i(t) = e^{-k_a t}, \quad [5]$$

The term $\partial Z_i(t)/\partial t$ represents the rate of removal of compound directly from the compartment. This includes the excretion of the compound from the body and the bioconversion of the substance into other compounds by metabolism. Metabolism is usually modeled using either linear kinetics

$$\frac{\partial}{\partial t}Z_i(t) = k_i V_i \quad [6]$$

or saturable nonlinear kinetics

$$\frac{\partial}{\partial t}Z_i(t) = V_{max}V_i/(K_m + V_i). \quad [7]$$

Here k_i is a first-order kinetic rate coefficient that can be estimated from metabolic studies. The parameter V_{max} is the maximum rate of metabolism under Michaelis–Menten kinetics, and K_m is an equilibrium constant that is numerically equal to the concentration of the substrate when the rate of metabolism is one-half of V_{max}. At low dose where the venous blood concentration V_i is less than K_m, the Michaelis–Menten Equation 7 can be approximated by a linear process as in Equation 6 with a rate coefficient of V_{max}/K_m. At high doses, the Michaelis–Menten equation approximates a zero-order process with $\partial Yi(t)/\partial t \approx V_{max}$.

The metabolism of methylene chloride involves both the linear (glutathione-*S*-transferase [GST]), pathway and the saturable (mixed-function oxidases [MFO]) pathway (10). Therefore, both removal processes (Equations 6 and 7) are required in the PBPK model for this compound.

With benzene, the first-generation metabolite (benzene oxide) is further metabolized into several phenol conjugates, phenyl mercapturic acid conjugates, and

hydroquinone conjugates. The generation of these secondary metabolites is considered as a separate process outside of the original five-compartment PBPK model for benzene (*11*).

Blood compartment

The mass–balance equation for the blood compartment takes a slightly different form from that in Equation 1 to satisfy the conservation of mass across all compartments. Specifically it is expressed as

$$\frac{\partial}{\partial t}C_b(t) = (1/U_b)\Sigma_i V_i(t) - (Q_b/U_b)C_b(t) + (1/U_b)\frac{\partial}{\partial t}Y_b(t) - (1/U_b)\frac{\partial}{\partial t}Z_b(t) \quad [8]$$

where $Q_b = \Sigma_i Q_i$, with Σ_i devoting the summation excluding the blood compartment.

For most compounds, the concentration in arterial blood leaving the blood compartment is the same as the blood concentration within the compartment. However, for TCDD, it is necessary to allow for binding to blood proteins. This effectively reduces the concentration in arterial blood flowing into different compartments (*7*).

Blood–Lung Compartment

For a volatile compound, the function of the lung must be included to represent the transfer of the compound between inhaled and exhaled air. The compartmental diagram in Figure 1 is then modified as shown in Figure 2, and the mass–balance equation in Equation 8 becomes:

$$\frac{\partial}{\partial t}C_b(t) = (Q_{alv}/U_b)(C_{inh}(t) - C_{alv}(t)) + (1/U_b)\Sigma_i Q_i V_i(t) - (Q_b/U_b)C_b(t) + (1/U_b)\frac{\partial}{\partial t}Y_b(t) - (1/U_b)\frac{\partial}{\partial t}Z_b(t) \quad [9]$$

where Q_{alv} is the alveolar ventilation rate, C_{inh} is the concentration of the compound in inhaled air, and C_{alv} is the concentration of the compound in alveolar tissue. The alveolar ventilation rate is easily obtained by direct measurement. The concentration of the compound in inhaled air and alveolar tissue can be expressed as

$$Ci_{nh}(t) = C_a(t) \quad [10]$$

and as:

$$C_{alv}(t) = P_a C_b(t) \quad [11]$$

respectively, where $C_a(t)$ denotes concentration in air, and P_a is air–blood partition coefficient.

A more complex representation of the blood–lung compartment has also been used in the study of methylene chloride to take into account metabolism in the lung, which is one of methylene chloride's target organs (*10*). The model uses one compartment to represent the exchange of methylene chloride between air and blood, and another to represent metabolism.

Selection of Physiologic Compartments

The body can be divided into two broad classes according to the value of the ratio U_i/Q_i in Equation 1. This ratio represents the period of time required to replace the volume of blood present in the ith compartment. The first class includes richly perfused tissues such as the liver and kidney; the second includes poorly perfused tissue such as skin and fat (*13*). Since metabolism in the liver represents a special function, it is usually considered as a separate compartment. Since fat will have much larger partition coefficient for lipophilic compounds, it may be considered as a separate compartment when studying fat-soluble substances. These considerations suggest the use of a PBPK model with the following five compartments: blood, liver, richly perfused tissue, poorly perfused tissue, and fat. For volatile compounds, the blood compartment may be replaced by a blood–lung compartment. With some variations, this basic five-compartment model has been widely used in PBPK modeling.

Solution of a PBPK Model

Consider the five-compartment PBPK model shown in Figure 3, in which the compound enters the blood compartment directly and is metabolized principally in the liver. The dynamics of this system are governed by the mass–balance equations representing the function of each compartment. If all of these equations are linear, then their solution can be expressed in closed form. More generally, the solution of both linear and nonlinear models can now be obtained using numeric methods. Computer programs such as Advance Continuous Simulation Language (ACSL)(*14*) and SIMUSOLV (*15*) specifically designed for this purpose are both efficient and easy to use.

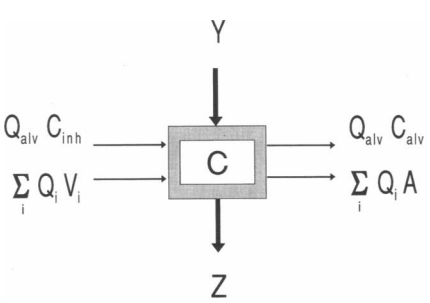

Figure 2. Schematic diagram of the blood–lung compartment.

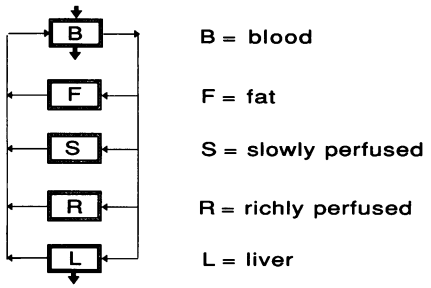

Figure 3. Schematic diagram of a five-compartment PBPK model.

To illustrate the solution of a PBPK model, consider the physiologic data in Table 1 for Sprague-Dawley rats previously reported by Leung et al. (*7*). Solutions to the five-compartment PBPK model shown in Figure 3 based on these values are illustrated in Figure 4 for the case of a single iv bolus injection of the test compound. The concentrations in each of the five compartments are shown in Figure 4A when there is no removal and all partition coefficients are equal to unity. In this case, the blood concentration is highest at the time of injection. As the compound is distributed to other compartments, the concentration in the blood decreases. At steady state, the concentration is the same in all compartments.

The richly perfused compartment has the smallest flushing time U_r/Q_r. Because the blood is being replaced quicker in this compartment than others, the concentration of the compound in the richly perfused compartment increases more rapidly than in other compartments. The concentration in this compartment reaches its peak when the venous and arterial blood

Table 1. Physiologic parameters of a Sprague-Dawley rat (*7*).

Compartment	Volume, liter	Blood flow, liter/hr	Time constant, hr
Blood	0.015	5.75	0.0026
Richly perfused	0.012	2.93	0.0041
Liver	0.015	1.44	0.0104
Fat	0.033	0.29	0.1149
Slowly perfused	0.213	1.09	0.1952

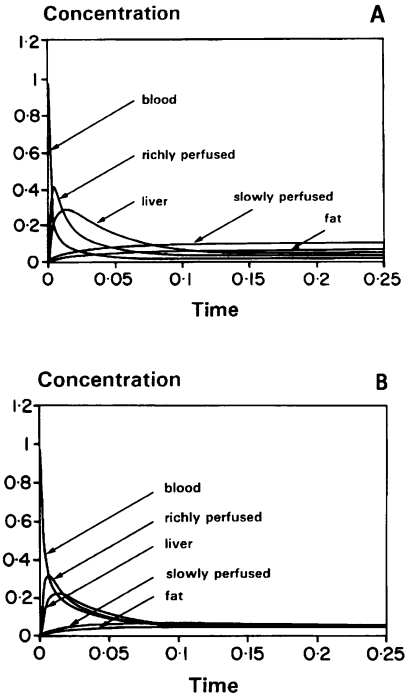

Figure 4. (*A*) Concentration in different compartments with no removal: P_r=, P_e=, P_s=, P_f = 1; (*B*) Concentration in different compartments with no removal: P_r = 2, P_t = 3, P_s = 5, P_f = 10.

concentrations are equal. Since the concentration in the blood compartment continually decreases because of distribution to other compartments, eventually the concentration in the richly perfused compartment surpasses that of the arterial blood. Consequently, the richly perfused compartment starts to release the compound back into the blood where it is transported to other compartments. Furthermore, since the richly perfused compartment is the first compartment whose venous blood concentration reaches that of the arterial blood, its peak concentration will exceed that in other compartments.

The compartment with the next smallest flushing time is the liver, in which the peak concentration is achieved after that of the richly perfused compartment. Both slowly perfused and fat compartments have large blood flushing times. Consequently, the concentration in these two compartments increases slowly. The peak venous blood concentration occurs at a much later time, and is smaller in amplitude. At steady state, the concentration in all compartments reaches the same equilibrium level.

When different partition coefficients are assigned to different compartments, the chemical flushing time $U_i P_i / Q_i$ assumes the role of the blood flushing time. The partition coefficients for blood and for richly perfused tissues are generally comparable, so that there is no change in the order in which compartments achieve their peak concentrations. However, the partition coefficient for fat can be much larger than that for slowly perfused tissue, so that the peak concentration in fatty tissue could occur at a much later time. The steady-state concentration in different compartments are proportional to their respective partition coefficients, as shown in Figure 4B.

The same model was modified to include saturable metabolism in the liver with K_m = 0.36 and V_{max} = 3.6 (in arbitrary units of measurement). Different doses 1, 10 and 100 are used to demonstrate the effect of saturation of removal. Figure 5 shows the concentration of the compound in the liver compartment, plotted on a semi-logarithmic scale. At the lowest dose, the venous blood concentration in liver is below K_m at all times, so that removal follows linear kinetics. At the middle dose, the venous blood concentration in the liver is above K_m near its peak. At this time, removal reaches its maximum rate and cannot proceed at a faster rate. At all other times, removal is essentially linear. Because of this saturation effect, the difference between the liver concentration at the low and middle dose is not consistent over time. With saturation of removal at the highest dose, more of the compound is retained in the liver. The differences among the three curves are therefore largest near their peaks.

Tissue Dosimetry

Some measure of the level of reactive metabolites reaching the target tissue should provide a better dose metameter for risk assessment purposes than the administered dose. However, consideration needs to be given to the most appropriate way to express tissue dose.

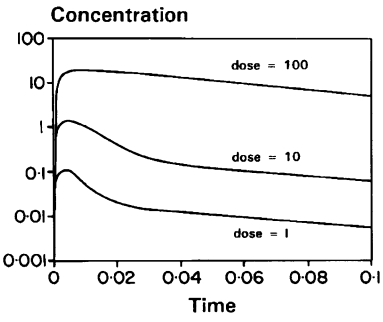

Figure 5. Liver concentration with saturable removal (V_{max} = 3.6, K_m = 0.36.

Integrated Tissue Dose

Andersen (*16*) used an integrated measure of tissue dose given by the area under the concentration–time curve (AUC) for either the parent compound or its reactive metabolites in the tissue concerned. Specifically, the AUC for the parent compound in blood is given by

$$AUC_b = \int_0^\infty C_b(t)\partial t. \quad [12]$$

For metabolites formed in the liver, we have

$$AUC_z = (1/U_t)\int_0^\infty \frac{\partial}{\partial t} Z_l(t)\partial t \quad [13]$$

which is simply the total amount of metabolite formed divided by the volume of the liver. The AUC in blood can be estimated directly by taking blood samples at frequent time intervals. However, this cannot be done in most other compartments, since tissue samples generally require destructive invasive sampling. Once a PBPK model has been developed, however, it can be used to predict tissue doses in any of the model compartments. Specific target tissues, if they are known, may be incorporated into the model as separate compartments.

For a linear PBPK model, the AUC of the parent compound in blood can be expressed as

$$AUC_b = \partial(1/Q_l + 1/k_l) \quad [14]$$

following administration of a single iv dose d of a xenobiotic. Note that this expression involves only the blood flow rate Q_l to the liver and the rate of metabolism k_l in the liver. The AUCs of the parent compound in other compartments are related to those in blood. Specifically, it can be shown that

$$AUC_l = P_l(AUC_b - d/Q_l) \quad [15]$$
$$AUC_r = P_r AUC_b \quad [16]$$
$$AUC_s = P_s AUC_b \quad [17]$$
$$AUC_f = P_f AUC_b \quad [18]$$
$$AUC_z = d/U_l. \quad [19]$$

Because of the relationship in Equation 2 between the concentration in a tissue compartment and venous blood leaving the compartment, the AUC for venous blood is the same for all compartments.

For a volatile compound with the blood compartment replaced by a blood/lung compartment, we have

$$AUC_b = d(1/Q_l + 1/k_l)G \quad [20]$$

where $G = 1/(1 + Q_{alv}P_a/(1/Q_l + 1/k_l))$. The

same factor G is applied to all other integrated doses given in Equations 15 to 19. This is similar to the steady-state solution for the metabolic clearance fraction given by Bogen (*17*).

Equations 15 to 18 provide simple relationships between the AUC in blood and other compartments. Since AUC_b can be determined directly from blood concentration measurements, these relationships could be used to predict the AUC in other compartments without constructing a complete PBPK model. Note that Equations 15 to 18 make no assumptions about the number of compartments included in the model, or the nature of metabolic processes (linear or saturable).

In a linear system, the only parameters which are important for the computation of the integrated dose are the blood flow rate to the liver Q_l, the removal rate of the compound in the liver k_l, and the partition coefficient P for the specific compartment. Other physiologic parameters such as tissue volume do not enter into the calculation. An increase in compartmental volume will increase the blood flushing time (as discussed previously) as well as delay the occurrence of the peak concentration and reduce amplitude. However, the AUC in that compartment remains unchanged.

The relative magnitudes of the AUCs in different compartments are determined solely by the partition coefficients. A change in the volume or blood flow rate in a compartment will only change the shape of the concentration–time curve, not the integrated tissue dose.

The integrated dose is dependent on the blood flow rate into the liver compartment. Because an increase in blood flow into the liver will increase the supply of the compound to liver tissue, and hence increase removal. Since the blood concentration declines monotonically following administration of a single iv dose, an increase in the rate of the change in the liver concentration will decrease AUC_l.

A compact solution for AUC_b similar to that in Equation 14 cannot be found for a nonlinear PBPK model. However, the simple relationships given in Equations 15 to 18 remain valid (*18*). Equation 20 now assumes the more complex form

$$\int_0^\infty (V_{max} C_l / (P_l + C_l)) \partial t = \partial \qquad [20]$$

Here the integrand is the rate of metabolism, and the integral on the left-hand side is the total amount of metabolite produced. This equation simply reflects the fact that the total amount of the metabolite produced should equal to the amount of the parent compound administered.

Sensitivity Analysis

From the systems analysis point of view, a PBPK model can be seen as a system where the level of exposure to a xenobiotic represents the input, and the dose of the reactive metabolite reaching the target tissue represents the output. The output relates to the input by means of a PBPK system that typically involves 20 or more parameters. Systems engineers often conduct analyses to determine how sensitive the model outputs are to changes in the values of the model parameters. Sensitivity analyses of this type offer a means of estimating the uncertainty in predictions of tissue doses conferred by uncertainty in the PBPK model parameters. Sensitivity analysis may also identify critical parameters that contribute most to the overall level of uncertainty in model outputs.

The first analysis of the uncertainty in PBPK model outputs was conducted by Portier and Kaplan (*19*). These investigators studied the PBPK model developed by Andersen et al. (*10*) for methylene chloride (DCM), which includes a total of 23 distinct parameters relating to tissue weights, blood flow rates, partition coefficients, and metabolic constants. Rather than focusing directly on the metabolites of methylene chloride reaching the lung and the liver, Portier and Kaplan (*19*) used the PBPK model predictions of metabolite concentrations in these two tissues to estimate the lifetime cancer risk due to exposure to methylene chloride. In this analysis, an essentially linear pharmacodynamic model was used to estimate cancer risks, with tissue doses expressed in terms of the area under the concentration–time curve in lung or liver for metabolites of DCM produced by the glutathione-*S*-transferase (GST) pathway.

Plausible ranges of uncertainty for the PBPK model parameters were based on published data when available; otherwise, coefficients of variation of the parameters were arbitrarily assigned values of 20 to 200%. Portier and Kaplan (*19*) reported that the variability in the 10^{-6} RSD (the dose estimated to increase the lifetime cancer risk by one in a million) was substantially greater allowing for uncertainty in the PBPK model parameters in comparison with treating these parameters as known constants. Specifically, the standard deviation of the distribution of RSDs was increased by a factor of about 10-fold.

Farrar et al. (*20*) conducted a similar uncertainty analysis for perchloroethylene using the PBPK model similar to that used in modeling styrene by Ramsey et al. (*21*). Because certain model parameters were not independent of one another, multivariate probability distributions were used to characterize prior information on parameter uncertainty. This study focused on three measures of tissue dose, namely the areas under the concentration–time curves for TCE in the liver and arterial blood, and the area under the concentration–time curve for metabolites of TCE in the liver. In addition, the variability in the RSD based on the induction of hepatocellular carcinomas was also considered. Although the results were generally supportive of the findings of Portier and Kaplan (*19*), these investigators concluded that the choice of an appropriate measure of tissue dose was of relatively greater importance for cross species extrapolation than uncertainty in PBPK model parameters.

Subsequent investigations have also provided useful information on uncertainty associated with predictions of tissue doses based on PBPK models. Hattis et al. (*22*) reported appreciable differences in predictions of the metabolism of perchloroethylene based on PBPK models constructed by seven different groups of investigators. Although there were some structural differences in the models used, the most important factor appeared to be the data used to calibrate metabolic parameters. Bois et al. (*23*) noted that three independently developed PBPK models for benzene provided noticeably different fits to the same data on benzene metabolism. It was further shown that acceptable fits to this data could be obtained with a relatively wide range of parameter values. Hetrick et al. (*24*) conducted a sensitivity analysis of PBPK models developed for styrene, methylchloroform, and methylene chloride. Predictions of tissue doses were shown to be particularly sensitive to the maximum rate of (Michaelis–Menten) metabolism and blood–air and blood–fat partition coefficients. The degree of sensitivity was shown to depend on the dose of the parent compound, the time at which tissue doses were predicted, and the species for which the PBPK model was developed.

Applications of PBPK Modeling

In the examples discussed below the resolution of many of the mechanisms involved in the uptake, distribution, metabolism and persistence of chemicals in the body

have been adequately resolved by the application of physiologically based models. Although some have been only partially resolved, the process of building a PBPK model often raises various questions that need to be addressed to elucidate pharmacokinetic mechanisms.

Methylene Chloride

The PBPK model for methylene chloride derives from a relatively simple model for volatile compounds originally developed for styrene (*10,21*). This perfusion-limited model incorporated five principal compartments: the lung, both as a compartment of excretion and, in some applications, the site of uptake; the liver, as the principal site of metabolism; richly perfused tissues, such as the kidney, brain and heart; slowly perfused tissues, such as muscle and skin; and fat, which could play an important role in storage and redistribution. Partition coefficients for blood and tissues were determined by *in vitro* techniques (*25,26*).

Metabolism of methylene chloride, measured by *in vitro* and *in vivo* techniques, was shown to proceed by two distinct pathways (*26,27*). One pathway involved the mixed-function oxidases (MFO) and the other was mediated by cytosolic GST. The MFO former pathway was found to be saturable in rats and mice at inhalation exposures of greater than about 200 ppm over a 6-hr period. The GST pathway was not saturable at concentrations up to 10,000 ppm over the same exposure period (*26*).

The delivered dose of the glutathione conjugated to the target tissues in rats and mice (liver and lung) and correlated better with carcinogenic response than did either the exposure dose or the products of metabolism by the mixed function oxidase pathway. *In vivo* and *in vitro* data from exposed humans and human tissues were used to calculate various estimates of cancer risk in humans. A comparison of the physiologically based pharmacokinetic model risk assessment data for liver tumors in humans showed that it was 168 times less than that calculated using the conventional U.S. Environmental Protection Agency (U.S. EPA) methodology, while the risk for lung tumors was 143 times greater using the U.S. EPA approach (*28,29*).

Ethylene Oxide

Ethylene oxide (EtO) is used in the sterilization of medical devices and as a fungicide in agriculture. It has also been identified as a human metabolite ethylene, a common air pollutant (*30*). In the evaluation of ethylene oxide as a carcinogen (*31,32*), the active carcinogenic species was considered to be ethylene oxide per se with the formation and elimination of metabolites representing a detoxification process (29).

The distribution of EtO was considered to be uniform throughout the body because of the similarity of tissue–blood partition coefficients in different compartments. It was also considered to be metabolized, principally by hydrolysis, to varying degrees in all compartments (*33*). Hydrolysis, without the intervention of enzyme catalysts, was shown to be followed by some degree of conjugation with glutathione (*34,35*). In addition, EtO has been shown to alkylate DNA and other biologic macromolecules (including hemoglobin) by direct interaction (*36,37*).

The physiologic model used to fit blood and tissue concentration data, was similar to that used for methylene chloride and styrene, except that the brain and testes were isolated from the richly perfused tissue compartment since these have been identified as target organs for EtO in animal studies (*38,39*). Rate constants for glutathione conjugation and DNA adduct formation were estimated from studies reported in the literature (*40,41*).

Data obtained in rats following iv administration and inhalation exposure allowed the simulation of ethylene oxide concentrations in target tissues as well as and the concentration of DNA and hemoglobin adducts. Experimental data following the iv administration of up to 100 mg/kg of EtO or after exposure to inhalation exposures to 1200 ppm for 6 hr did not appear to demonstrate biochemical thresholds; whole body elimination of ethylene oxide appeared to follow first-order kinetic process. However, this analysis facilitated the identification and characterization of the hydrolysis of EtO, glutathione conjugation, exhalation, and DNA or hemoglobin binding. These latter processes were affected by saturation of elimination pathways at high-exposure concentrations where the whole body elimination continued to follow first-order kinetics (*33*). Information on the metabolic capacity of human tissues for the hydrolysis and glutathione conjugation of ethylene oxide would greatly facilitate the extrapolation of animal cancer risk estimates to humans.

1,4-Dioxane

1,4-Dioxane has been used for decades as an industrial solvent. Aside from inducing hepatic and renal effects it has also been shown to induce liver tumors in rodents and to induce nasal carcinomas in rats (*42–44*). Young et al. (*45*) showed that the metabolism of 1,4-dioxane was saturable at high doses.

Two recent reports on the application of physiologically based pharmacokinetics of 1,4-dioxane (*8,46*) incorporated the kinetic constants for the formation of the principal metabolite (β-hydroxy ethylacetic acid). The model accommodated the administration of 1,4-dioxane by the iv, inhalation, and oral routes and allowed the calculation of the surrogate delivered doses to various organs, particularly the liver. Metabolic thresholds were observed at water concentrations of greater than 1% administered by the oral route and at atmospheric concentrations of greater than 300 ppm inhaled continuously (*8*). These investigators suggested that unless the physiologic and metabolic differences between humans and rats were corrected for, human cancer risk based on traditional risk assessment methods applied to the administered dose would be overestimated.

1-Nitropyrene

1-Nitropyrene, a nitrated polycyclic aromatic hydrocarbon, has been detected in diesel exhaust emissions, coal combustion products, and photocopier toners (*47–49*). 1-Nitropyrene is closely related to the class of compounds known as polycyclic aromatic hydrocarbons, many of which are known carcinogens. The systemic uptake, metabolism and excretion of 1-nitropyrene has been shown to be very rapid with wide distribution to body tissues (*50*).

1-Nitropyrene is a potent bacterial and mammalian mutagen, and induces lung tumors in mice and mammary tumors in rats following subcutaneous injection (*51–53*). Tumors were also found at the injection site.

Medinsky et al. (*54*) developed a PBPK model for 1-nitropyrene incorporating the principal organs to which 1-nitropyrene was distributed, metabolized and bound (namely the upper respiratory tract, lung, liver, and kidney). This model provided a good description of the clearance of metabolites via the bile and feces as well as through urine. Partition coefficients for the lung, liver and kidneys relative to blood were found to be close to unity, indicating that consideration of blood flow alone is sufficient to describe the clearance of 1-nitropyrene from these tissues. This model appeared to provide a good description of the doses of 1-nitropyrene and its metabolites to target tissues, as well as their temporal relationship postexposure.

Polychlorinated Biphenyls, Dioxins, and Furans

These classes of chemicals represent a major group of ubiquitous and persistent environmental pollutants that have been a cause of great concern for the past several decades (*55*). While the mechanisms involved in the toxicity of these groups of chemicals are still under investigation, immune alterations and decreased specific antibody response (*56,57*) have been noted for the chlorinated biphenyls and 2,3,7,8-tetrachlorodibenzo-*p*-dioxin (TCDD) (*58,59*). The polychlorinated biphenyls tend to act as hepatocarcinogens (*44,60*) induces liver tumors in rats and is cocarcinogenic (*61,62*).

The toxicity of the dioxins and furans differs markedly among species (*63,64*) as does their pharmacokinetics and disposition (*65,66*). The chlorinated dibenzodioxins and dibenzofurans accumulate in the liver and adipose tissue, although there are notable species differences in their relative distribution to these tissues (*67*). This may be due in part to binding at different sites, such as the *Ah* locus, in responsive and nonresponsive different species (*68–70*).

The PBPK models proposed for polychlorinated biphenyls (*12,71*), 2,3,7,8-tetrachlorodibenzo-*p*-dioxin and 2,3,7,8-tetrachlorodibenzofurans (*65,66,72,73*) are all rather similar. They generally involve five or six compartments, consisting of the blood, slowly perfused tissues, and richly perfused tissues with separate compartments for the principal target tissues: fat and liver.

For hexachlorobiphenyl, the model was able to describe blood level data adequately following the administration of a single iv dose in the rat (*12*). Since this compound is excreted very slowly, blood concentrations were followed for 43 days postdosing. Growth, particularly of the fat compartment, was incorporated into the model. The rate of conversion to, and excretion of, the glucuronide conjugate via the bile was taken into account. Enterohepatic recycling was considered to be important. The authors expressed the opinion that the variables in the model had been adequately assessed and that species and route variations could be accommodated to describe the delivered dose to specific target tissues.

For the polychlorinated dibenzodioxins and dibenzofurans, bile rather than urine was considered to be the major route of excretion. The liver is a major site of toxic action of these agents. Liver–blood partition coefficients were very large, ranging between 30 and 130 for the various rodent and primate species considered. Microsomal enzyme induction and binding to the Ah receptor sites were accommodated in the PBPK model. Since the arylhydrocarbon hydroxylase complex has been implicated in the carcinogenic mechanism(s) for these compounds, it has been suggested that the PBPK model could be useful for cancer risk assessment (*7,65,72–74*).

Other Considerations in Applications of PBPK Models

The development of a PBPK model for a particular compound may require special consideration of factors other than those involved in the applications described in the previous section. One of the benefits of building a PBPK model is increased understanding of the pharmacokinetic processes involved in the distribution and elimination of xenobiotics. The examples that follow illustrate the need for enhanced PBPK modeling to accommodate the effects of growth and aging, topical adsorption, pregnancy, and competitive multiple metabolites.

Animal Aging and Body Growth

In the studies of the pharmacokinetics of polychlorinated biphenyls discussed earlier (*12,71*), it was found that hexachlorobiphenyl is excreted very slowly by the rat. At 6 weeks, postdosing, over 80% of the iv dose was retained, and the fraction that was excreted in the urine and feces comprised mainly of metabolites. Over this time period the rats, originally weighing between 250 and 300 g, gained appreciable body weight. Since fat increases proportional to total body weight when the animal grows, hexachlorobiphyl in poorly perfused fat tissue became increasingly diluted during the experiment. Thus, fat concentrations beyond 8 days postdosing were not well predicted without the incorporation of an adjustment for the increase in the volume of the fat compartment as a function of age.

A similar circumstance arose in attempts to fit data obtained from pharmacokinetic and tissue disposition studies of methyl chloroform in young and old rodents (*75,76*). To fit the data obtained from old (18.5 months) rats, it was necessary to increase the size of the fat compartment from 7% (for young, 1- to 3-month-old rats) to 18% of their body weight. The concentration of methylchloroform in body fat was 20 to 100 times greater than that in any other tissue. Thus the model predicted that the increased size of the fat compartment in older animals would increase the amount taken up. The model also predicted that methyl chloroform would be more slowly released in younger animals than in older animals. The same integrated model was found to be applicable to data derived from iv administration, inhalation, bolus gavage, and administration in drinking water, as well as data obtained with repeated doses (*8*).

Topical Adsorption in Inhalation Studies

Inhalation studies of volatile chemicals have usually carried out by placing the whole animals in a carefully controlled exposure chamber. In the closed chamber technique (*77,78*) inferences about the kinetics of uptake and disposition of volatile chemicals are made by monitoring the change in chamber concentration with time.

In studying the kinetics of chlorinated ethane in rats, Gargas and Anderson (*79*), encountered a high loss (78%/hr) of ethanes containing three or more chlorine atoms from empty chambers. This turned out to be primarily due to adsorption to carbon dioxide adsorbents and to the inner chamber surface. While these effects could be measured and satisfactorily incorporated into the PBPK model, the concentration of 1,1,2,2-tetrachloroethane, in the chamber immediately following exposure, was underestimated by nearly an order of magnitude.

Since the excess chamber concentration could be accounted for only as an additional amount carried to the chamber passively by the animal, it was assumed that tetrachloroethane was adsorbed extensively to the fur of the animals. This hypothesis was confirmed by exposing rats to 350 ppm of tetrachloroethane for 6 hr in an exposure chamber. The animals were then given a lethal dose of sodium pentobarbital and placed singly in an exhaled breath chamber with the chamber atmosphere monitored for tetrachloroethane. Since the animals were not breathing, it was assumed that the atmospheric concentrations of tetrachloroethane could only have been derived from the desorption of the chemical from the fur of the animal. This experiment allowed the derivation of the amount of the chemical adsorbed on the fur and a first-order rate coefficient was determined for desorption from the fur. When the fur adsorption/desorption data was used in conjunction with exhaled breath analysis, the PBPK provided an adequate fit of the live animal data.

Pregnancy, Lactation, and Nursing

Many changes occur during pregnancy that can have a significant impact on the toxicodynamics of a particular chemical. For

example, the changes in body weight, total body water, plasma proteins, body fat, and cardiac output will alter the distribution of many xenobiotics (*80–82*).

PBPK models have been used to describe the kinetics and disposition of the drugs tetracyline, morphine, and methadone (*83–85*). Two recent reports described the pharmacokinetics and disposition of trichloroethylene and its principal metabolite, trichloroacetic acid, in the pregnant rat as well as the lactating rat and nursing pup. A PBPK model consisting of eight compartments for trichloroethylene in the pregnant rat and nine compartments for trichloroacetic acid was used (*86*). Both models accommodated multiple routes of exposure and repeated dosing. The model provided for a variable litter size 1 to 12 pups per rat as well as placental growth.

Values of the maximum rate of metabolic removal velocity (V_{max}) in naive and pregnant rats were 10.98 and 9.18 mg/kg/hr, respectively. This reduction is significant, and has been related to a decrease in the cytochrome P450 monooxygenase activity due to altered steroid hormones. A high substrate affinity was demonstrated. Although the value of the Michaelis constant (K_m) was low (0.25 mg/l), it was similar in both groups of rats. Fetal exposure to trichloroethylene was estimated to range from 67 to 76% of the maternal exposure; fetal exposure to the trichloroacetic acid metabolite was 63 to 64% of that of the dam.

The model-fitted data obtained after exposure by the inhalation, oral gavage, or by drinking water. Other kinetic parameters predicted by the model (such as the relative volumes of distribution, the peak blood concentration following oral gavage, fetal concentrations following inhalation exposure, absorption, and elimination rates) agreed well with previous data reported in the literature. These results demonstrated that fetal exposure to both the parent compound and its principal metabolite was significantly elevated in relation to the maternal exposure.

Fisher et al. (*87*) examined the transfer of trichloroethylene and trichloroacetic acid to nursing pups from lactating dams exposed to trichloroethylene by inhalation of 610 ppm, 4 hr/day, 5 days/week from days 3 to 14 of lactation. A further study involved exposure of the lactating dam to 333 mg/ml of trichloroethylene in drinking water from days 3 to 21 of lactation. The exposure of the pups to trichloroethylene was solely from ingested maternal milk; however, their exposure to trichloroacetic acid derived from maternal milk and from metabolism of ingested trichloroethylene. The model provided for different values during lactation for compartmental volumes, blood flows, and milk yield obtained from the published literature. Metabolic and other kinetic parameters were determined experimentally.

The values of V_{max} = 9.26 mg/kg/hr in the lactating rat was similar to that in the pregnant rat. However, the value of V_{max}= 12.94 mg/kg/hr obtained for male and female pups indicated that the ability of the pups to metabolize trichloroethylene was greater than that of the adult. The plasma half-life (16.5 hr) of trichloroacetic acid in the pups was also substantially greater than that of the mature rat. Unlike most other physiologic distribution processes which are flow limited, the distribution of trichloroacetic acid to mammary tissue is diffusion limited. The exposure of the pups to trichloroethylene from maternal milk was small, representing only about 2% of the exposure of the dam. Pup plasma levels of trichloroacetic acid; however, were as high as 30 and 15% of the maternal exposure for drinking water and inhalation exposures, respectively.

Mixtures

The interaction between two or more chemicals is a very complex phenomenon involving chemical interactions prior to absorption, competition for a common metabolic pathway, and competition for sites of toxic action (*88*). Each of these processes could be a consequence of other complex mechanisms that have seldom been defined completely.

One example, in which PBPK modeling has been used to describe the quantitative interaction between two compounds metabolized by the same microsomal oxidation pathway is that of trichloroethylene and 1,1-dichloroethylene (*89*). 1,1-Dichloroethylene was shown to induce acute hepatoxicity as a consequence the reactivity of their metabolic products. The metabolic pathway was the same for both compounds, and there was high-affinity substrate binding which was saturable (*90*). Coexposure of rats to 1,1-dichloroethylene and vinyl chloride dramatically reduced the hepatoxicity of the former (*91*).

A PBPK model was developed, assuming competitive inhibition by both compounds, to estimate the hepatoxicity of 1,1-dichloroethylene in the absence and presence of trichloroethylene. Elevated liver enzymes provided a pharmacodynamic index of hepatotoxicity. In rats exposed to 0, 200, 300, and 400 ppm of dichloroethylene alone, it was observed that the serum glutamic oxaloacetic transaminase (SGOT) enzyme level increased dramatically at exposures above 100 ppm. When animals were exposed to 300, 713, and 1718 ppm of 1,1-dichloroethylene and 500 ppm of trichloroethylene, the SGOT elevation was significantly reduced. This behavior was consistent with purely competitive inhibition with binding constants of 0.25 mg/l for trichloroethylene and 0.10 mg/l for 1,1-dichloroethylene. It was evident that 1,1-dichloroethylene is a slightly better substrate for microsomal oxidation than trichloroethylene. The model was able to predict the combined pharmacodynamic effects of these two substrates when coadministered in any proportion.

Pharmacodynamics

Chemical carcinogenesis is a complex process involving a number of steps, which may include biotransformation of the parent compound to its reactive metabolites, DNA damage, mutation, proliferation of mutated cells, progression to a malignant state, and growth of malignant tissue to overt tumors (*66,92*). The two-stage clonal expansion model of carcinogenesis, originally developed by Moolgavkar and Venzon (*93*) and Moolgavkar and Knudson (*94*) provides a convenient framework for describing the process of carcinogenesis. The model is based on the premise that two critical mutations are required to convert a normal stem cell to a malignant cancer cell; the effects of cell kinetics are reflected in the birth and death rates of stem cells as well as initiated cells which have sustained the first mutation.

The dose of the proximate carcinogen to the target tissue can impact the process of neoplastic transformation in several ways. The probability of either a first- or second-stage mutation can be increased by direct alkylation of DNA at the time of cell division. Mitogenic compounds which increase the rate at which stem cells divide can also increase the mutation frequency by increasing the opportunity for either spontaneous or induced mutation. Once a genetic lesion induced in a stem cell has been fixed by replication, promoting agents may augment the size of the iniated cell population by selective clonal expansion of initiated cells. Increasing the pool of initiated cells increases the number of cells at risk of sustaining the second critical mutation, which completes the process of neoplastic conversion. This two-stage model of carcinogenesis is no doubt an over-

simplification of the process of neoplastic transformation. Nonetheless, it does embody critical factors such as mutation, tissue growth, and cell kinetics involved in carcinogenesis, and has proven useful in modeling dose–response relationships observed in toxicologic and epidemiologic studies (*1*).

An important consideration in such applications is the manner in which dose in incorporated into the modeling process. In most applications, the external level of exposure to the host has been used in predicting cancer risk. The use of the external level of exposure in dose–response modeling can lead to biases in predictions of low-dose cancer risks when the relationship between the administered dose level and the dose of the reactive metabolite reaching the target tissue is nonlinear (*95*). Physiologic models offer an approach to tissue dosimetry which can be used to avoid such biases.

PBPK models permit calculation of various measures of tissue dose. With a given chemical carcinogen, the mechanisms of interaction between dose and tissue constituents and the mechanisms by which these interactions lead to cancer will determine the proper measure of tissue dose for risk assessment calculations. Within the framework of the two-stage model, increases in either mutation rates or growth rates of normal or intermediate cells can lead to increased cancer risk. It follows that the interaction of the toxicant with target tissue must have cellular consequences that are eventually reflected in alterations in the rates of one or more of these processes.

Mechanistic information has been used to suggest a very broad brush classification of chemical carcinogens (*92*). Genotoxic carcinogens interact directly with DNA bases to form promutagenic adducts which alter mutational probability during cell division. Nongenotoxic carcinogens do not interact directly with DNA; rather, they alter cell division rates. These alterations can either be due to direct mitogenic stimulation of the tissue or indirectly as a reparative process following tissue cytotoxicity. Because all carcinogens interact with cells leading to formation of genotypically altered cells and must therefor have some genotoxic sequelae, the terms DNA reactive and non-DNA reactive have also been suggested as a more appropriate than genotoxic/nongenotoxic. Another proposal is the differentiation between genotoxic and operationally nongenotoxic carcinogens. In general DNA reactive carcinogens are initiators and the non-DNA reactive chemicals are promoters. The mechanism of toxicant–tissue interaction specifies the linkage between dosimetry of these individual carcinogens and the rates of mutation or of proliferation of normal and altered cells involved in tumor formation. The linkage between tissue dose and these cellular parameters for three broad classes of chemical carcinogens is examined below.

DNA Reactive Chemicals

Certain electrophiles react with nucleophilic sites on DNA bases to form promutagenic adducts. Chemicals such as ethylene oxide, propylene oxide, dimethylmethylsulfonate, and bis-chloronitrosourea react directly with these bases (*96,97*). Other chemicals such as nitrosamines, vinyl chloride, and aflatoxins have to be metabolized in the body to form reactive electrophiles (*96*). In either case, tumor formation is believed to be associated with changes in mutation probabilities related to the production and persistence of adducts. The adducts are generally expected to be formed by second-order reactions and removed by saturable repair enzymes. For a chemical like ethylene oxide (EtO), the equation for the rate of change in the amount of tissue adducts over time t is (*33*):

$$V\partial[\text{DNA–EtO}]/\partial t = k[\text{EtO}][\text{DNA}]\,V_{max} - V_{max}–[\text{DNA–EtO}]/(K_m+[\text{DNA–EtO}]) \quad [22]$$

Here, [EtO], [DNA], and [DNA–EtO] denotes the concentration of EtO, DNA, and DNA–EtO adducts in the target tissue with volume V. The parameter k represents the second-order rate constant at which adducts are formed, with V_{max} and K_m denoting the Michaelis–Menten parameters for (saturable) enzymatic repair.

With this model, [DNA–EtO] can be used as a surrogate for increases in probability of mutation in each cell division event. Highly reactive chemicals will form several different adducts and the mutational efficacy will vary for each of these individual adducts. However, if all processes are linear, the increased mutational rates would still be expected to be linearly related to the integrated tissue exposure to EtO. In this case, the cumulative exposure of the target tissue to the critical reactive metabolite may be used as a measure of tissue dose. Other factors need to be considered in interspecies extrapolation. For example, it is unclear whether risk across species for DNA reactive chemicals should be normalized based on integrated daily dose or on integrated lifetime dose. In either case, the tissue dose metameter is the integrated tissue dose of DNA reactive electrophile integrated over an appropriate period of the animal or human life-span.

Non-DNA Reactive Cytoxic Chemicals

With non-DNA reactive chemicals, the initial cellular interactions are frequently associated with accumulation of sufficient doses of highly reactive species to cause cell death. The parent compound may be reactive, as with formaldehyde in the nasal mucosa or ethyl acrylate and ethylene dichloride in forestomach (*97,98*). In other cases, the chemical is converted to reactive metabolites in the target tissues: chloroform, carbon tetrachloride, and vinylidene chloride kill hepatocytes only after metabolism to phosgene, trichloromethyl free radical, and chloroacetylchloride, respectively (*99–101*). The mechanisms of toxicant–target tissue interaction vary depending on the chemical nature of the reactive intermediate. Some reactive chemicals form long-lived stable adducts with cellular proteins and lipids. Examples include carbon tetrachloride and acetaminophen (*99,102*). The depletion of critical tissue macromolecules below critical levels then leads to cell death. For carbon tetrachloride (CCl_4), a reactive trichloromethyl free radical ($\cdot CCl_3$) covalently binds to macromolecules. The two equations relating tissue–macromolecule [tissue–MM] concentrations include terms for MM synthesis (k_0), MM degradation (k_1), loss of MM due to a second-order reaction with reactive chemical (k_2), accumulation of the tissue–CCl_3 adducts from the second-order reaction, and degradation of the adducts (k_3):

$$\partial[\text{Tissue}-\text{MM}]/\partial t = K_0 - k_1[\text{Tissue–MM}] - k_2[\cdot CCl_3][\text{Tissue–MM}] \quad [23]$$

and

$$\partial[\text{Tissue}-CCl_3]/\partial t = k_2[\cdot CCl_3][\text{Tissue–MM}] - k_3[\text{Tissue}–CCl_3] \quad [24]$$

The concentration of free radicals should be related to the reaction rate divided by the tissue volume (*10*). In this example, biologic factors such as the MM synthesis rate and degradation rate constant of adducted protein and lipid are important factors in interspecies extrapolation. Cell death is expected to be associated with reduction of tissue MM below critical levels for some period of time. A PBPK model of CCl_4 has been used to estimate tissue burdens of bound reactive metabolite in rats (*103*), although it has not yet been applied in a risk assessment calcula-

tion. *Cis*-platin, a cancer chemotherapeutic agent, forms protein adducts which have a cell half-life similar to the cell half-life estimated for the CCl_3 adducts from carbon tetrachloride. Farris et al. (*104*) have developed a detailed PBPK model of *cis*-platin that describes adducts with both low molecular weight and high molecular weight peptide constituents in cells. Unlike $CHCl_3$ which does not react appreciably with DNA, *cis*-platin cytotoxicity is believed to be related causally to its cross-linking with DNA that interferes with cell replication.

With $CHCl_3$, a PBPK model has been developed to estimate cell killing under various exposure conditions in rats and mice (*105*). $CHCl_3$ is metabolized to short-lived intermediates, phosgene and hydrochloric acid, which are highly irritant, but whose adducts are not persistent (*106*).

Cell death was more closely associated with high rates of metabolism over relatively short times then to persistence of macromolecular adducts (*105,107*). An empirical approach was taken to describe the relationship between the rate of death of normal hepatocytes ($-\partial Nh/\partial t$) and the rate of metabolism per unit volume of tissue ($\partial Amet/\partial t)/V$). The rate of loss of hepatocytes was modeled with a rate constant for cell death (K_{death}), the number of viable hepatocytes at any time (Nh), and a distribution of sensitivities to cell killing ($SENS$) that was based on the rate of metabolism per unit tissue volume:

$$\partial(Nh)/\partial t = -K_{death}(SENS)(Nh). \quad [25]$$

The sensitivity distribution described the proportion of cells at risk at any rate of chloroform metabolism in the cell and was derived empirically from appropriate experiments. In the absence of chronic tissue injury, cell replication should restore the tissue to normal functional status. The cell replication rate should mirror the death rate with some delay. The replication rate affects the overall mutation rate, which corresponds to the product of mutation probability per cell division and the rate of cell division.

Many chemicals will resist such simple classification, and demonstrate characteristics shared by multiple categories. Nitrosamines are highly mutagenic, but are also cytolethal at high doses. These chemicals alter both mutational and replicative processes in cells in the target tissues (*108*). The mutational efficacy persists even at doses below which there is little cell killing. Formaldehyde is cytolethal and produces DNA–formaldehyde–protein cross-links which probably have mutagenic potential (*109*). The exposure response relationships for both processes are nonlinear with similar shapes. The mutation rate for chemicals with cytotoxic and DNA reactive characteristics should be related to the product of replication rate times the level of cross-links; the increases in replication rate should affect other cell growth parameters as well (*110*).

Non-DNA Reactive Mitogenic Chemicals

It is difficult to define the action of this diverse class of carcinogens by a single mechanism. These compounds appear to promote tumor development primarily by increasing cell replication in the two-stage cancer model, and frequently by selective enhancement of replication in preneoplastic instead of normal tissue. Many of these chemicals act via receptor molecules to modulate expression of protein growth factors. Examples include dioxin, dioxinlike polyhalogenated biphenyls and dibenzofurans, peroxisomal proliferators, phenobarbital, and phenobarbitallike PCBs, as well as various hormones and hormone-analogs. The relevant measure of biologic dose leading to cell replication is the alteration in concentration of protein-growth regulatory products. The relevant measure of tissue dose of chemical must be related to interactions between the chemical and the receptor molecules responsible for regulating expression of these growth factors.

PBPK models for dioxin have attempted to link dioxin tissue concentrations, receptor action, and expression of particular genes. To date, the models account for expression of certain metabolizing proteins, cytochrome P4501A1 (CYP1A1) and cytochrome P4501A2 (CYP1A2), but not for induction of specific sets of growth factors. Dioxin interacts with a cytosolic protein, the Ah receptor, and the dioxin-receptor complex translocates to the nucleus and, together with at least one other protein factor, binds to specific sites on DNA to modulate transcription of various genes (*59,111*). Several receptor-based models linking tissue dioxin and gene regulation have been described. Initially, induction was calculated by estimating the fractional occupancy of the Ah receptor, as determined based on an Ah receptor–dioxin binding constant, and the tissue concentration of dioxin and Ah receptor (*46,112*). More recently, this induction model has been extended in an attempt to account for ternary interactions involving the binding of the dioxin–Ah receptor complex to sites on DNA and the possibility of cooperative interactions among multiple DNA binding sites for this complex in regulatory regions of specific genes (*112*). The relationships modeled include the binding of dioxin and Ah receptor, cooperative binding of the receptor-dioxin complex to DNA sites, and the increased synthesis rate of protein consequent to the alterations in gene transcription. The two relevant relationships become

$$[\text{Dioxin–Ah}] = [\text{Dioxin}][\text{Ah receptor}]/K_b \quad [26]$$

and

$$\partial[\text{CYP1A1}]/\partial t = K_0 + K_{max}[\text{Dioxin–Ah}]^n/([\text{Dioxin–Ah}]^n + K_d^n) - K_1[\text{CYP1A1}]. \quad [27]$$

Here, K_b is the dioxin–Ah receptor dissociation constant, K_0 is the basal synthesis rate of CYP1A1, K_{max} is the fully induced CYP1A1 synthesis rate, n is a Hill coefficient interpreted as reflecting the cooperative binding of the Ah receptor-dioxin complex to regulatory regions of DNA, K_d is the dissociation constant for the DNA–dioxin–Ah complex, and K_1 is the degradation rate constant for the CYP1A1 under normal conditions. To be of use in risk assessment, these models will ultimately have to predict the regulation of sets of growth regulatory genes in an attempt to model the proliferative responses directly. In the interim, the induction of specific gene products, such as CYP1A1 and CYP1A2, can be used to develop correlations with carcinogenic sequelae of these promoters, bearing in mind that there is no reason to expect a causal relationship between these cytochrome activities and tumor formation.

Summary and Conclusions

In this article, we have reviewed the development and application of PBPK models as a tool for estimating the dose of reactive metabolites of chemical carcinogens reaching target tissues. In general terms, PBPK models envisage the body as being comprised as a small number of relatively homogeneous physiologic compartments. Such models are characterized mathematically by a system of mass–balance equations that can be readily solved using modern computer software to obtain predictions of tissues doses. However, the development and applications of a PBPK model is not a trivial undertaking.

Information on all of the allometric, biochemical, and pharmacokinetic parameters involved in the model must be developed, and the model validated and refined by appropriate experimentation. This process can generate significant insight into the uptake, distribution, metabolism, and elimination of xenobiotics suspected of increasing cancer risk.

From the risk assessment point of view, the primary goal of PBPK modeling is to obtain more accurate estimates of cancer risk through the use of more accurate measures of tissue dose. While the use of more relevant measures of dose is likely lead to progress towards this objective, the uncertainty associated with predictions of tissue dose must not be overlooked. This uncertainty can be evaluated by considering the precision associated with each of the model parameters, and by identifying those parameters to which predictions of tissue dose are most sensitive.

Complete, quantitative biologically motivated models for carcinogenic risk assessment must ultimately include several components: a PBPK description for tissue dosimetry, a linking model specifying the mechanism by which tissue dose interacts with cell constituents to produce alterations in cell growth rates or mutation probabilities during replication, and the impact of alterations in these cellular events on tumor promotion. Significant progress is evident in development of PBPK models and in investigating model sensitivity and the impact of parameter variability on risk calculations (*19,23,113,114*). The two-stage model is a promising quantitative description of the relationship between cellular events and cancer which can be expanded as new information on the obligate mutational events in chemical carcinogenesis for specific carcinogens becomes known in more detail (*93,115,116*). The greatest challenge today is the further elaboration of these linkage processes that are important in transducing chemical interactions into direct biologic consequences. Perhaps the most tangible reward expected from improved quantitative linking models is the more precise definition of the measure of tissue dose and the possibility of better definition of the manner in which these measures of tissue dose should be normalized across species for various mechanisms of action to support informed interspecies extrapolations.

The work required to develop these comprehensive, biologically motivated risk assessment models including their validation with specific experiments under long-term chronic exposure conditions is expected to be costly and time-consuming. Clearly, it is impossible to create these models for every chemical. A more reasonable, cost-effective strategy may be to invest in models for a limited number of chemicals with well-defined mechanisms of action in order to create prototype risk assessment approaches for generic classes of chemicals of widespread interest. With these prototype chemicals, model development early on in the process of toxicity testing can guide subsequent experimental design for validating, refuting, or refining current modeling methodologies. These linking models are now in their formative stages, and more work will be required to improve the biologic basis of these descriptions and test various assumptions. Their very existence, though, will help refine and focus succeeding research efforts and improve the likelihood that research will find more fruitful the process of quantitative risk assessment for chemical carcinogens.

REFERENCES

1. Krewski D, Withey JR, Ku LF, Travis CC. Physiologically based pharmacokinetic models:applications in carcinogenic risk assessment. N Trends Pharmacokin 355–390 (1991).
2. U.S. EPA. Guidelines for carcinogenic risk assessment. Fed Reg 51. Washington:U.S. Environmental Protection Agency, 1986; 33993–34014.
3. Travis CC, White RK. Interspecies scaling of toxicity data. Risk Anal 8:119–126 (1988)
4. Goddard MG, Krewski D. Interspecies extrapolation of toxicity data. Risk Anal 12, 315–317 (1992).
5. Arms AD, Travis CC. Reference Physiological Parameters in Pharmacokinetic Modelling. EPA/600/6-88/004. Washington: U.S. Environmental Protection Agency, 1988.
6. Andersen ME. Physiological modeling of organic compounds. Ann Occup Hyg 35:309–321 (1991).
7. Leung HW, Paustenbach DJ, Murray FJ, Andersen ME. A physiological pharmacokinetic description of the tissue distribution and enzyme-inducing properties of 2,3,7,8-tetrachlorodibenzo-*p*-dioxin in the rat. Toxicol Appl Pharmacol 103:399–410 (1990).
8. Reitz RH, McCroskey PS, Park CN, Andersen ME, Gargas ML. Development of a physiologically based pharmacokinetic model for risk asessment with 1,4-dioxane. Toxicol Appl Pharmacol 105:37–54 (1990).
9. Medinsky MA, Sabourin PJ, Lucier G, Birnbaum LS, Henderson RF. A physiological model of simulation of benzene metabolism by rats and mice. Toxicol Appl Pharmacol 99:193–206 (1989).
10. Andersen ME, Clewell III HJ, Gargas ML, Smith FA, Reitz RH. Physiologically based pharmacokinetics and the risk assessment process for methylene choride. Toxicol Appl Pharmacol 87:185–205 (1987).
11. Medinsky MA, Sabourin PJ, Lucier G, Birnbaum LS, Henderson RF. A physiological model for simulation of benzene metabolism by rats and mice. Toxicol Appl Pharmacol 99:193–206 (1989).
12. Lutz RJ, Dedrick RL, Matthews HB, Eling TE, Anderson MW. A preliminary pharmacokinetic model for several chlorinated biphenyls in the rat. Drug Metab Dispos 5(4):386–396 (1977).
13. Fiserova-Bergerova V. Physiological models for pulmonary administration and elimination of inert gases. In: Modelling of Inhalation Exposure to Vapors. Uptake, Distribution, and Elimination (Fiserova-Bergerova V, ed). Boca Raton,FL:CRC Press, 1983;73–100.
14. Advanced Continuous Simulation Language (ACSL) Reference Manual. Mitchell & Gauthier Associates (MGA), 1992.
15. Steiner EC, Blau GE, Agin LA. Introductory Guide to Simusolv, Modeling and Simulation Software. The Dow Chemical Company, Midland, MI, 1989.
16. Andersen ME. Saturable metabolism and its relationship to toxicity. Crit Rev Toxicol 9:105–150 (1981).
17. Bogen KT. Pharmacokinetics for regulatory risk analysis: the case of trichloroethylene. Regul Toxicol Pharmacol 8:447–466 (1988).
18. Krewski D, Wang Y, Ku LF. Calculation of the area under the concentration–time curve in physiologically based pharmacokinetic models. Laboratory for Research in Statistics and Probability, Technical Report. Carleton University, Ottawa, Canada, 1994.
19. Portier CJ, Kaplan NL. Variability of safe dose estimates when using complicated models of the carcinogenic process. Fundam Appl Toxicol 13:533–544 (1989).
20. Farrar D, Allen B, Crump K, Shipp A. Evaluation of uncertainty in input parameters to pharmacokinetic models and the resulting uncertainty in output. Toxicol Lett 49:371–385 (1989).

21. Ramsey JC, Andersen ME. A physiologically based description of the inhalation pharmacokinetics of styrene in rats and humans. Toxicol Appl Pharmacol 73:159–175 (1984).
22. Hattis D, White P, Marmorstein L, Koch P. Uncertainties in pharmacokinetic modeling for perchloroethylene. I. Comparison of model structure, parameters, and predictions for low-dose metabolism rates for models derived by different authors. Risk Anal 10(3):449–458 (1990).
23. Bois FY, Woodruff TJ, Spear RC. Comparison of three physiologically based pharmacokinetic models of benzene disposition. Toxicol Appl Pharmacol 110:79–88 (1991).
24. Hetrick DM, Jarabek AM, Travis CC. Sensitivity analysis for physiologically based pharmacokinetic models. J Pharmacokin Biopharm 19(1):1–20 (1991).
25. Sato A, Nukajima T. Partition coefficients of some aromatic hydrocarbons and ketones in water, blood and oil. Br J Ind Med 36:231–234 (1979).
26. Gargas ML, Clewell III HJ, Andersen ME. Metabolism of inhaled dihalomethanes *in vivo*: differentiation of kinetic constants for two independent pathways. Toxicol Appl Pharmacol 82:211–223 (1986).
27. Ahmed AE, Anders MW. Metabolism of dihalomethanes to formaldehyde and inorganic halode. I. *In vitro* studies. Drug Metab Dispos 4:357–361 (1978).
28. U.S.EPA. Update to the health assessment document and addendum for dichloromethane: pharmacokinetics, mechanism of action and epidemiology. EPA 600/-87/-030. Cincinnati, OH:U.S. Environmental Protection Agency, 1987.
29. Krishnan K, Gargas ML, Fennell TR, Andersen ME. Ethylene oxide risk assessment: incorporating dosimetry and mechanistic information. Activities, Chemical Industry Institute of Toxicology 11:1–8 (1991).
30. Tornqvist M, Gustaffson B, Kantiainen A, Harms-Ringdahl M, Granath F, Ehrenberg L. Unsaturated lipids and intestinal bacteria as sources of endogenons production of ethene and ethylene oxide. Carcinogenesis 10:39–41 (1989).
31. Lynch DW, Lewis TR, Moorman W, Burg JR, Grath DH, Khan A, Acherman LJ, Cockrell BY. Carcinogenic and toxicologic effect of ethylene oxide and propylene oxide in Fischer-344 rats. Toxicol Appl Pharmacol 76:69 (1984).
32. Snellings WM, Weil CS, Maronpot RR. A two year inhalation study of carcinogenic potential of ethylene oxide in Fischer-344 rats. Toxicol Appl Pharmacol 75:105–117 (1984).
33. Krishnan K, Gargas ML, Fennell TR, Andersen ME. A physiologically based pharmacokinetic description of ethylene oxide dosimetry in the rat. Toxicol Ind Health 8:121–140 (1992).
34. Jones AR, Wells G. The comparative metabolism of 2-bromoethanol and ethylene oxide in the rat. Xenobiotica 11:763–770 (1981).
35. Tardif R, Goyal R, Brodeur J, Gerin M. Species differences in the urinary disposition of some metabolites of ethylene oxide. Fundam Appl Toxicol 9:448–453 (1987).
36. Fost U, Marczynski B, Kaseman R, Peter H. Determination of 7-(2-hydroxethyl) guanine with gas chromatography/mass spectrometry as a parameter for genotoxicity of ethylene oxide. Arch Toxicol 13:250–253 (1989).
37. Segerback D. Reaction products in hemoglobin and DNA after *in vitro* treatment with ethylene oxide and *N*-(2-hydroxyethyl) nitrosurea. Carcinogenesis 11:307–312 (1990).
38. Garman RH, Snellings WM, Masonpot RR. Frequency, size and location of brain tumours in F-344 rats chronically exposed to ethylene oxide. Food Chem Toxicol 24:145–153 (1986).
39. Florack EIM, Zielhins GA. Occupational ethylene oxide exposure and reproduction. Int Arch Occup Environ Health 62:273–277 (1990).
40. Zemaitis MA, McKelvey JA. The effects of ethylene oxide exposure on tissue glutathione levels in rats and mice. Drug Chem Toxicol 9:51–66 (1986).
41. Potter D, Blair D, Davies R, Watson WP, Wright AS. The relationship between alkylation of hemoglobin and DNA in Fischer 344 rats exposed to ^{14}C-ethylene oxide. Arch Toxicol 13:254–257 (1989).
42. Argus MF, Sohal RS, Bryant GM, Hoch-Ligeti C, Arcos JC. Dose-response and ultrastructural alterations in dioxane carcinogenesis. Eur J Cancer 9:237–243 (1973).
43. Kociba RJ, McCollister SB, Park CN, Torkelson TR, Gehring PJ. 1,4-Dioxane. I. Results of a two year ingestion study in rats. Toxicol Appl Pharmacol 30:275–286 (1974).
44. National Cancer Institute. Bioassay of Arochlor 1254 for Possible Carcinogenicity. NCI-GC-TR-30. Bethesda, MD:National Cancer Institute, 1978.
45 Young JD, Brann WH, Ghong PJ. The dose-dependent fate of 1,4-dioxane in rats. J Environ Pathol Toxicol 2:263–282 (1978).
46. Leung HW, Poland A, Paustenbach DJ, Murray FJ, Andersen ME. Pharmacokinetics of [^{125}I]-2-iode-3,7,8-trichlorodibenzo-*p*-dioxin in mice: analysis with a physiological modeling approach. Toxicol Appl Pharmacol 103:411–419 (1990).
47. Pitts Jr JN, Lokensgard DM, Harger W, Fischer TS, Mena V, Schuller JJ, Scorziel GM, Katenstein YA. Mutagens in diesel exhaust particulates, identification and direct activities of 6-nitrobenzo[*a*]pyrene, 9-nitroanthracene, 1-nitropyrene and ^{5}H-phenanthro[4,5-bed]pyran-5-one. Mutat Res 103:241–249 (1982).
48. Hanson RL, Henderson TR, Hobbs CH, Clark CR, Carpenter RL, Dutcher JC. Detection of nitroaromatic compounds on coal combustion particles. J Toxicol Environ Health 11:791-800 (1983).
49. Rosenkranz HS, McCoy EC, Sanders DR, Butler M, Kiriazides DK, Mermelstein R. Nitropyrenes: isolation, identification, and reduction of mutagenic impurities in carbon black and toners. Science 209:1039–1043 (1980).
50. Bond JA, Sun JD, Medinsky MA, Jones RK, Yeh HC. Deposition, metabolism and excretion of 1-^{14}C-nitropyene and 1-^{14}C-nitropyrene coated on diesel exhaust particles as influenced by exposure concentration. Toxicol Appl Pharmacol 86:102–117 (1986).
51. El-Bayoumy K, Hecht SS, Sackl I, Stoner GD. Tumorgenicity and metabolism of 1-nitropyrene in A/J mice. Carcinogenesis 5:1449–1452 (1984).
52. Hirose M, Lee MS, Wang CY, King CM. Induction of rat mammary gland tumors by 1-nitropyrene, a recently recognized environmental mutagen. Cancer Res 44:1158–1162 (1984).
53. Ohgaki H, Matsukura N, Morino K, Kawachi T, Susimura T, Morita K, Tokiwa H, Hirota T. Carcinogenicity in rats of the mutagenic compounds 1-nitropyrene and 3-nitrofluoranthrene. Cancer Lett 15:1–7 (1982).
54. Medinsky MA, Bond JA, Hunsberger S, Griffith Jr WC. A physiologically based model of 1-nitropyrene metabolism after inhalation or ingestion. Health Phys 57(Suppl 1):149–155 (1989).
55. Hutzinger O, Safe S, Zitko V. The Chemistry of the PCB's. Cleveland:CRC Press, 1974.
56. Chang KJ, Ching JS, Huang PC, Tung TC. Study of patients with PCB poisoning. J Formosan Med Assoc 79:304–312 (1980).
57. Loose LD, Silkworth JB, Pittman KA, Benitz KF, Mueller W. Impaired host resistance to endotoxin and malaria in polychlorinated biphenyl and hexachlorobenzene treated mice. Infect Immun 20:30–35 (1978).
58. U.S. EPA. Health assessment document for polychlorinated dibenzo-*p*-dioxins. EPA-600-8-84-OMF. Cincinnati, OH:U.S. Environmental Protection Agency, 1985.
59. Safe SH. Comparative toxicology and mechanisms of action of polychlorinated dibenzo-*p*-dioxins and dibenzofurans. Annu Rev Pharmacol Toxicol 26:371–399 (1986).
60. Ito N, Nagasaki H, Arai M, Makiura S, Sugihara S, Hirao, K. Histopathologic studies on liver tumorigenesis induced in mice by technical polychlorinated biphenyls and its promoting effect on liver tumors induced by benzene hexachloride. J Natl Cancer Inst 51:1637–1646 (1973).
61. Toth K, Somfai-Relle S, Sugar J, Bence J. Carcinogenicity testing of herbicide 2,4,5-trichlorophenoxyethanol containing dioxin and of pure dioxin in Swiss mice. Nature 278:548–549 (1979).

62. Kouri RE, Rude TH, Joglekar R, Dansette PM, Jerina DM, At SA, Owens IS, Nebert DW. 2,3,7,8-Tetrachlorodibenzo-p-dioxin as cocarcinogen causing 3-methylcholanthrene-initiated subcutaneous tumors in mice genetically "nonresponsive" at *Ah* locus. Cancer Res 38(9):2777–2783 (1978).
63. Schwet BA, Noris JM, Sparschu GL, Rowe VK, Gerhing PJ, Emerson JL, Gervig CG. Toxicology of chlorinated dibenzo-*p*-dioxins. Environ Health Perspect 5:87–100 (1973).
64. Moore JA, McConnell EE, Dalgard DW, Harris MW. Comparative toxicity and halogenated dibenzofurans in guinea pigs, mice and rhesus monkeys. Ann N Y Acad Sci 320:151–163 (1979).
65. Leung HW, Ku RH, Paustenbach DJ, Andersen ME. A physiologically based pharmacokinetic model for 2,3,7,8-tetrachlorodibenzo-*p*-dioxin in C57BL/6J and DBA/2J mice. Toxicol Lett 42:15–28 (1988).
66. King FG, Derick RL, Collins JM, Matthews HB, Birnbaum LS. Physiological model for the pharmacokinetics of 2,3,7,8-tetrachlorodibenzofuran in several species. Toxicol Appl Pharmacol 67:390–400 (1983).
67. Byard JL. The toxicological significance of 2,3,7,8-tetrachlorodibenzo-*p*-dioxin and related compounds in adipose tissue. J Toxicol Environ Health 22:381–403 (1987).
68. Poland A, Glover E, Glende AS. Stereospecific high affinity binding of 2,3,7,8-tetrachlorodibenzo-*p*-dioxin by hepatic cytosol. J Biol Chem 251:4936–4946 (1976).
69. Gasiewicz TA, Geiger TA, Rucci G, Neal RA. Distribution, excretion and metabolism of 2,3,7,8-tetrachlorodibenzodioxin in C57BL/6J, DBA/2J and B6D2F,/J mice. Drug Metab Dispos 11:397–403 (1983).
70. Neal RA. Mechanisms of the biological effects of PCBs, polychlorinated dibenzo-*p*-dioxins and polychlorinated dibenzofurans in experimental animals. Environ Health Perspect 60:41–46 (1985).
71. Bungay PM, Dedrick RL, Matthews HB. Pharmacokinetics of halogenated hydrocarbons. Ann NY Acad Sci 257–270 (1979).
72. Leung HW, Paustenbach DJ, Andersen ME. A physiologically based pharmacokinetic model for 2,3,7,8-tetrachlorodibenzo-*p*-dioxin. Chemosphere 18(1–6):659–664 (1989).
73. Kissel JC, Robarge GM. Assessing the elimination of 2,3,7,8-TCDD from humans with a physiologically based pharmacokinetic model. Chemosphere 17(10):2017–2027 (1988).
74. Andersen ME, Greenlee WF. Biological basis for risk assessment of dioxins and related compounds (Banbury Report 35) (Gallo MA, Scheuplein RJ, van der Heijden KA, eds). Cold Spring Harbor, NY:Cold Spring Harbor Laboratory Press, 1991;379–388.
75. Schumann AM, Fox TR, Watanabe PG. C-Methyl choroform (1,1,1-trichloroethane): pharmacokinetics in rats and mice following inhalation exposure. Toxicol Appl Pharmacol 62:390–401 (1982).
76. Reitz RH, McDougal JN, Himmelstein MW, Nolan RJ, Schumann AM. Pharmacokinetics of inhaled styrene in human volunteers. Toxicol Appl Pharmacol 53:54–63 (1988).
77. Filser JG. The closed chamber technique - uptake, endogenous production, excretion, steady-state kinetics and rates of metabolism of gases and vapors. Arch Toxicol 66:1–10 (1992)
78. Andersen ME, Gargas ML, Jones RA, Jenkins Jr LJ. Determination of the kinetic constants of metabolism of inhaled toxicants *in vivo* based on gas uptake measurements. Toxicol Appl Pharmacol 54:100–116 (1980).
79. Gargas ML, Andersen ME. Determining kinetic constants of chlorinated ethane metabolism in the rat from rates of exhalation. Toxicol Appl Pharmacol 99:344–353 (1989).
80. Hytten FE, Chamberlain G. Clinical Physology in Obstetrics. Oxford:Blackwell Press, 1980.
81. Mattison, D.R. Drug and Chemical Action in Pregnancy (Fabro S, Scialli AR, eds). New York:Marcel Dekker,1986.
82. Mattison DR, Blann E, Malek A. Physiological alterations during pregnancy: impact on toxicokinetics. In: Symposium on Pharmacokinetics in Developmental Toxicity. Fundam Appl Toxicol 16:215–218 (1991).
83. Olanoff LS, Anderson JM. Controlled release of tetracycline III: a physiologically pharmacokinetic model of the pregnant rat. J Pharmacokin Biopharm 8:599–620 (1980).
84. Gabrielson JL, Poalzow LK. A physiological pharmacokinetic model for morphine disposition in the pregnant rat. J Pharmacokin Biopharm 11:147–163 (1983).
85. Gabrielson JL, Johansson P, Bondesson U, Poalzoe LK. Analysis of methadone disposition in the pregnant rat by means of a physiological flow model. J Pharmacokin Biopharm 13:355–372 (1985).
86. Fisher JW, Whittaker TA, Clewell III HJ, Andersen ME. Physiologically based pharmacokinetic modeling of the pregnant rat: a multiroute model for trichloroethylene and its metabolite trichloroacetic acid. Toxicol Appl Pharmacol 99:395–414 (1989).
87. Fisher JW, Whittaker TA, Taylor DH, Clewell III HJ, Andersen ME. Physiologically based pharmacokinetic modeling of the lactating rat and nursing pup: a multiroute exposure model for trichloroethylene and its metabolite, trichloroacetic acid. Toxicol Appl Pharmacol 102:497–513 (1990).
88. Calabrese EJ. Multiple Chemical Interactions. Chelsea, MI:Lewis Publishers, 1991.
89. Andersen ME, Gargas ML, Clewell HJI, Severyn KM. Quantitative evaluation of the metabolic interactions between trichloroethylene and 1,1-dichloroethylene *in vivo* using gas uptake methods. Toxicol Appl Pharmacol 89:149–157 (1987).
90. Andersen ME, French JE, Gargas ML, Jones RA, Jenkins Jr LJ. Saturable metabolism and the acute toxicity of 1,1-dichloroethylene. Toxicol Appl Pharmacol 47:395–409 (1979)
91. Jaeger RJ, Conolly RB, Murphy SD. Short-term inhalation toxicity of halogenated hydrocarbons. Arch Environ Health 30:36 (1975).
92. Butterworth BE. Consideration of both genotoxic and nongenotoxic mechanisms in predicting carcinogenic potential. Mutat Res 239:117 (1990).
93. Moolgavkar SH, Venzon DJ. Two event models for carcinogenesis: incident cancer hv childhood and adult tumors. Mathematical Bios 47:55–77 (1979).
94. Moolgavkar SH, Kinderson AG. Mutation and cancer: a model for human carcinogenesis. J Natl Cancer 66:1037–1052 (1981).
95. Krewski D, Murdoch DJ, Withey JR. The application of pharmacokinetic data in carcinogenic risk assessment. Pharmacokinetics in Risk Assessment. Drinking Water and Health 8:441–468 (1987).
96. Ehrenberg L, Moustacchi E, Osterman-Golkar S, Ekman G. Dosimetry of genotoxic agents and dose–response relationships of their effects. Mutat Res 123:121–182 (1983).
97. Kroes R, Webster PW. Forestomach carcinogens: possible mechanisms of action. Food Chem Toxicol 24:1083–1089 (1986).
98. Webster PW, Kroes R. Forestomach carcinogens: pathology and relevance to man. Toxicol Pathol 16:165–171 (1988).
99. Recknagel RO, Glende EA, Ugasio G, Koch RR, Srinvasan S. New data in support of the hepatotoxicity of carbon tetrachloride liver injury. Isr J Med Sci 10:301–311 (1974).
100. Recknagel RO. Carbon tetrachloride hepatotoxicity. Pharmacol Rev 19:145–208 (1967).
101. Henschler D. Metabolism and mutagenicity of halogenated olefins—a comparison of structure and activity. Environ Health Perspect 21:61–64 (1977).
102. Jollow DJ, Mitchell JR, Potter WE, Davis DC, Gillette JR, Brodie BB. Acetaminophen-induced hepatic necrosis II. J Pharmacol Exp Ther 187:195–202 (1973).
103. Paustenbach DJ, Clewell III HJ, Gargas ML, Andersen ME. A physiologically based pharmacokinetic model for inhaled carbon tetrachloride. Toxicol Appl Pharmacol 96:191–211 (1988).
104. Farris FF, Dedrick RL, King FG. *Cis*-platin pharmacokinetics: applications of a physiological model. Toxicol Lett 43:117–137 (1988).
105. Reitz RH, Mendrala AL, Corley RA, Quast JF, Gargas ML, Andersen ME, Staats DA, Conolly RB. Estimating the risk of liver cancer associated with human exposures to chloroform using physiologically based pharmacokinetic modeling. Toxicol Appl Pharmacol 105:443 (1990).
106. Ilett KK, Reid WD, Sipes IG, Kirshna R. Chloroform toxicity

in mice: correlation of renal and hepatotoxicity with covalent binding of metabolites to macromolecules. Exp Mol Pathol 19:215–229 (1973).
107. Corley RA, Mendrala AL, Smith FA, Staats DA, Gargas ML, Conolly RB, Andersen ME, Reitz RH. Development of a physiologically based pharmacokinetic model for chloroform. Toxicol Appl Pharmacol 103:512–527 (1990).
108. Travis CC, McClain TW, Birkner PD. Diethylnitrosamine induced hepatocarcinogenicity in rats: a theoretical study. Toxicol Appl Pharmacol 109:289–304 (1991).
109. Casanova M, Morgan KT, Steinhagen WH, Everitt JI, Popp JA, Heck H D'A. Covalent binding of inhaled formaldehyde to DNA in the respiratory tract of rhesus monkeys: pharmacokinetics, rat-to-monkey interspecies scaling and extrapolation to man. Fundam Appl Toxicol 17:409–428 (1991).
110. Conolly RB, Monticello TM, Morgan KT, Andersen ME, Monticello TM, Clewell HJ. A biologically based risk assessment strategy for inhaled formaldehyde. Comm Toxicol 4:269–294 (1992).
111. Poland A, Knutson JC. 2,3,7,8-Tetrachlorodibenzo-*p*-dioxin and related halogenated aromatic hydrocarbons: examination of the mechanisms of toxicity. Annu Rev Pharmacol Toxicol 22:517 (1982).
112. Andersen ME, Mills JJ, Gargas ML, Kedderis L, Birnbaum LS, Neubert D, Greenlee WF. Modeling receptor-mediated processes with dioxin:implications for pharmacokinetics and risk assessment. Risk Anal 13:35–36 (1993).
113. Cohn MS. Sensitivity analysis in pharmacokinetic modeling. Drinking Water and Health 7:265–272 (1987).
114. Bois FY, Zeise L, Tozer TN. Precision and sensitivity of pharmacokinetic models for cancer risk assessment: tetrachloroethylene in mice, rats and humans. Toxicol Appl Pharmacol 102:300–315 (1990).
115. Moolgavkar SH, Knudson AG. Mutation and cancer: a model carcinogenesis. J Natl Cancer Inst 66:1037–1052 (1981).
116. Conolly RB, Reitz RH, Clewell III HJ, Andersen ME. Biologically structured models and computer simulation: application to chemical carcinogenesis. Comm Toxicol 2:305 (1988).